

Molecular Imprinting Electrochemical Sensor for Sensitive Creatinine Determination

Zhenyu Zhang¹, Yang Li², Xiaoqin Liu¹, Yanhui Zhang² and Dongmei Wang^{3,*}

¹ Department of Nephrology, Hongqi Hospital Affiliated to Mudanjiang Medical University, Mudanjiang, Heilongjiang, 157000, P.R. China

² Department of Orthopedic Surgery, Hongqi Hospital Affiliated to Mudanjiang Medical University, Mudanjiang, Heilongjiang, 157000, P.R. China

³ Department of Laboratory Medicine, Hongqi Hospital Affiliated to Mudanjiang Medical University, Mudanjiang, Heilongjiang, 157000, P.R. China

*E-mail: dongmeiwang3@163.com

Received: 1 November 2017 / *Accepted:* 14 January 2018 / *Published:* 5 February 2018

Creatinine has been considered indicative of renal condition measurement after a dialysis. In the present work, a silver nanoparticles (AgNPs)/polyoxometalate functionalized reduced graphene oxide (rGO) coated glassy carbon electrode (GCE) based molecular imprinted voltammetric biosensor was for the first time prepared for the analysis of creatinine. XRD and X-ray photoelectron spectroscopy (XPS) measurements were used for the characterization of the modified surface. The limit of detection (LOD) was obtained as 1.51×10^{-11} M, with a linear range of 0.05-1.5 nM. And the developed biosensor has been used for the detection of real specimens with desirable stability, recovery and selectivity.

Keywords: Molecular imprinting; Electrochemical sensor; Creatinine; Renal disease; Saliva

1. INTRODUCTION

Renal diseases are a main contributing factor for mortality and morbidity (prevalence: 17.2%). As a global concern, it is urgent to study its early detection, evaluation, progression delay through some preventative treatment, along with adverse outcome prevention. Around the world, the number of people living on dialysis reaches more than 1 million. During the past 15 years, the renal failure incidence has been doubled [1, 2]. The filtration rate of glomerular is reduced lower than 15 ml/min in the case of progressive renal failure, which results in imbalanced serum electrolytes and accumulated metabolic byproducts including creatinine and urea. Therefore it is urgent to perform renal

replacement therapy (RRT) so as to prevent severe detrimental complications. On the other hand, the constant timely hemodialysis performed at regular intervals can substitute RRT to sustain life for the patients with chronic renal failure [3-5].

The initiating time for dialysis or dialysis frequency has been recognized as two important factors in homeostasis maintaining and life quality improvement for these patients. It is necessary to constantly monitor the levels of metabolic byproducts in serum, including potassium, creatinine, and urea. The infection risks of patients could be increased by repeated venipuncture [6, 7]. Through paracellular or transcellular routes, different molecules enter saliva, which is normally regarded as a blood filtrate. Therefore, saliva is indicative of the physiological state of the body as the serum [8-10]. Based on literature, the renal failure patients show different salivary level of creatinine [11-13]. In the present work, receiver operator characteristic (ROC) curve and diagnostic validity test were used to study the detection accuracy of salivary creatinine, based on the improved salivary diagnostic systems. On the other hand, the cutoff values for salivary levels of creatinine were also obtained.

Currently, a spectrophotometric strategy based on the classic Jaffé reaction between alkaline picrate and creatinine has been regarded a common method for the analysis of creatinine [14-17]. Based on the specificity study of the Jaffé spectrophotometric strategy in many different reports [18-20], interfering effects by drugs and endogenous species have been reported. Thus for the renal patients care in the world, it is urgent to develop a highly accurate technique for the routine analysis of creatinine. In the healthy adult males sera, the reference concentration of creatinine ranges from 79.5 to 123.7 μM ; for females, it is a little bit lowered: 70.5–106.1 μM . On the other hand, the daily output of urinary creatinine for males ranges from 9.7 to 24.7 mmol, and 7.9–14.1 mmol for females.

Previous works have reported some electrochemical strategies, such as potentiometric biosensors, for the routine detection of creatinine [21-24]. Unfortunately, the above potentiometric sensors have been proved less sensitive, and prone to be interfered in the presence of endogenous ammonia in physiological specimens. Compared with conventional potentiometric biosensors, the amperometric creatinine biosensors are more favorable, ascribed to the high sensitivity, rapid response, and low LOD.

To transform the host–analyte interaction into a readable signal output, physicochemical transducers were coupled with molecular recognition materials. Electrochemical methods possess some merits, including instrumentation portability, low-cost, and miniaturization, thus having gained extensive study among numerous transduction strategies [25, 26]. Recently a majority of biosensors are label-dependent sensors based on secondary functional electroactive/photoactive molecules. However, there are also label-free biosensors with excellent operational simplicity and rapidness, such as SPR and QCM [27]. For biomarker analysis, the label-free biosensors have also been developed using another low-cost and fast method [28, 29]; in addition, the hand-held and cost-effective impedance analyzers could also be accessed. In this report, the molecular imprinted gold nanoelectrode ensembles were applied to the creatinine detection.

2. EXPERIMENTS

2.1. Chemicals

Activated carbon, sulphuric acid (H_2SO_4), potassium permanganate (KMnO_4), hydrogen peroxide (H_2O_2), isopropyl alcohol (IPA), ethanol, MeCN, silver nitrate (AgNO_3), graphite powder, creatinine, phenol, and T $\text{H}_3\text{PW}_{12}\text{O}_{40}$ (POM) were commercially available in Sigma–Aldrich (USA). Sodium acetate, acetic acid, phosphorus pentoxide (P_2O_5), and potassium persulfate ($\text{K}_2\text{S}_2\text{O}_8$) were commercially available in Merck (Germany).

2.2. Characterizations

IVIUMSTAT & IVIUMSTAT.XR: Electrochemical Interface & Impedance Analyzer was used for electrochemical impedance spectroscopic (EIS) measurements. A C3 cell stand equipped IviumStat (U.S) was used to obtain cyclic voltammograms (CV) and Differential pulse voltammograms (DPV). XRD experiments were carried out using a Rigaku Mini X-ray diffractometer. XPS patterns were obtained using PHI 5000 Versa Probe (Φ ULVAC-PHI, Inc., Japan/USA), with monochromatized Al $\text{K}\alpha$ radiation (1486.6 eV) as an X-ray anode operated at 50 W.

2.3. Synthesis of rGO, POM/rGO and AgNPs/POM/rGO

The synthesis of GO was carried out based on our reported study [30]. A suspension with a yellow-brown color was obtained after dispersing the above GO into 200 mL water under mild ultrasonic treatment. Then the obtained suspension was mixed with 4 mL 80 wt% hydrazine hydrate, followed by 1 d heating treatment under oil bath kept at 100 °C under a water-cooled condenser. The product obtained after the completion of reaction was filtered under vacuum rGO to yield rGO product. This was followed by dissolving the obtained rGO into 2 mg/mL ethanol, and ultrasonically agitated for 60 min. On the other hand, a ultra-violet (UV) light source was used for the reduction of 1 mL of 1 mM $\text{H}_3\text{PW}_{12}\text{O}_{40}$. Then the reduced POM was added to the obtained rGO suspension at a volume ratio of 1:1 for 120 min to yield POM/rGO. In a quartz bottle, 0.4 mg/mL POM/rGO solution was mixed with 1 mM AgNO_3 solution at a volume ratio of 1:1. Then a homogeneous suspension was yielded after the mixture was sonicated. This was followed by 40 min stirring under the UV light. And the coated electrode was obtained after dropping AgNPs/POM/rGO (20 μL) onto the bare GCE, i.e., AgNPs/POM/rGO modified GCE, which was then left drying under an infrared heat lamp.

2.4. Fabrication of creatinine imprinted voltammetric sensor

rGO/GCE, POM/rGO/GCE and AgNPs/POM/rGO/GCE were obtained after dropping rGO, POM/rGO and AgNPs/POM/rGO suspensions (15 μL) on the clean bare GCE, respectively. This was followed by the evaporation of solvent using an infrared lamp. With phenol (100 mM) in pH 6.0 phosphate buffer solution (PBS) + creatinine (25 mM), 20 cycles of CV were run to obtain the

creatinine imprinted surface on AgNPs/POM/rGO/GCE (MIP/AgNPs/POM/rGO/GCE), potential range: 0.6 V to +1.5 V, scan rate: 50 mV/s [31]. Under the same procedure, the creatinine non-imprinted surface (NIP) was prepared in the absence of OCH. Electrostatic interactions between monomer and OCH molecules can be found, along with the hydrogen bonding between them. The above reactions were terminated using a NaCl solution (1.0 M). The creatinine imprinted electrode was firstly dipped into the desorption agent (30 mL), followed by 10 min electrode swinging under a 100 rpm bath. Then the OCH was removed, and the sensor was left drying under nitrogen gas.

3. RESULTS AND DISCUSSION

The deposition of POM on rGO sheets was carried out through electron transfer and electrostatic interactions between POM and the rGO sheets, resulting in a heterogeneous catalyst [32]. XPS measurements were also carried out to study the preparation of AgNPs/POM/rGO. As displayed in Fig. 1, the peaks of C_{1s}, Ag_{3d}, O_{1s} and W_{4f} provided evidence that AgNPs/POM/rGO has been formed. The peaks observed at 282.5 eV, 284.3 eV and 285.2 eV were associated with the C–H, C–N and –CONH of C_{1s} core-level spectrum, respectively [33, 34]. For the AgNPs/POM/rGO, the band of 372.4 eV was associated with the Ag 3d^{3/2}, 366.5 eV with Ag 3d^{5/2}, which provided evidence that AgNPs was present [35].

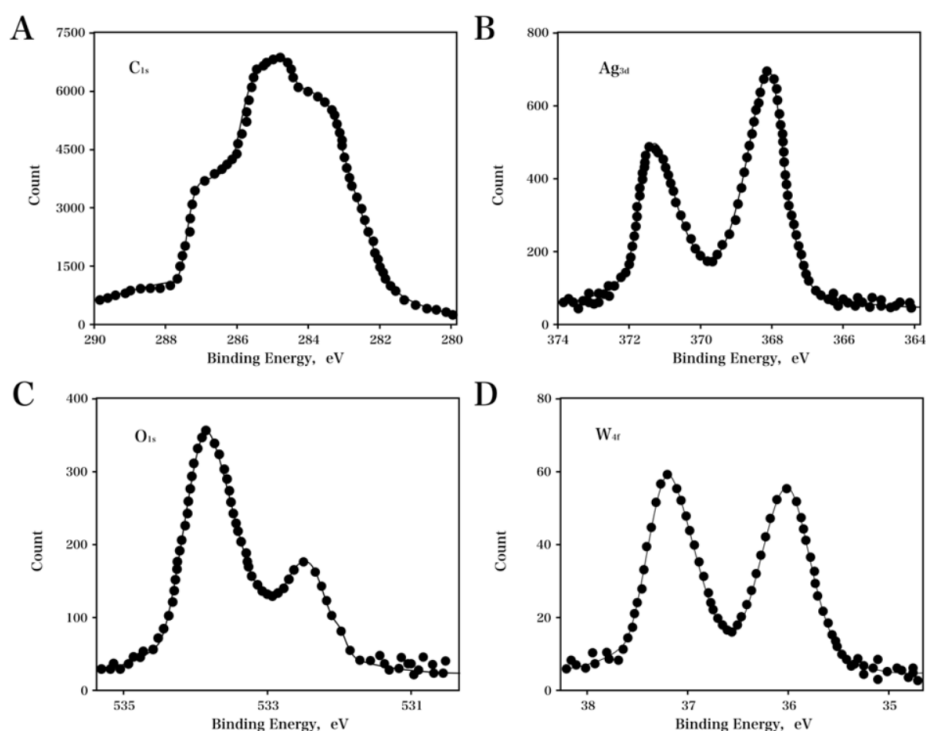


Figure 1. XPS spectra of (A) C 1s, (2) Ag 3d, (C) O 1s and (D) W4f of AgNPs/POM/rGO.

Fig. 2 showed the XRD characterization of AgNPs/POM/rGO nanohybrid. The narrow and intense peaks observed at $2\theta = 33.33^\circ$ and 43.25° were associated with the (002) and (004) planes of rGO sheets, respectively. The peaks observed at $2\theta = 36.10^\circ$ and 45.23° were associated with the (111) and (200) planes of Ag, respectively. On the other hand, the peaks observed at $2\theta = 25.04^\circ$, 27.12° , 37.03° and 42.91° were associated with the (442), (642), (555) and (953) planes of POM, respectively [36-38].

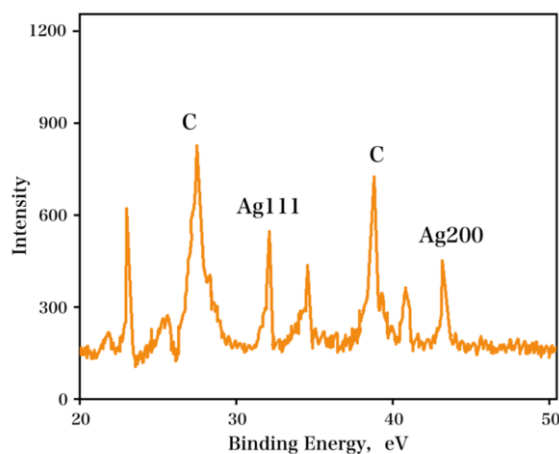


Figure 2. XRD pattern of AgNPs/POM/rGO.

For the bare GCE, the charge transfer resistance (R_{ct}) was obtained as 114Ω , as shown in the EIS characterization in curve a (Fig. 3A). A low R_{ct} was shown as 72Ω for the rGO coated GCE, which suggested no charge transfer rate decrease was caused by the presence of rGO. The POM/rGO coated GCE showed lower R_{ct} value than rGO/GCE. Thus, the addition of silver nanoparticles shows an increase in the active surface area and the catalytic activity. An almost straight line was shown for AgNPs/POM/rGO coated GCE (EIS), suggesting that the electrochemical process was diffusion limited [39-41].

As displayed in curve a of Fig. 3B, R_{ct} was obtained as 676Ω for the MIP/AgNPs/POM/rGO coated GCE upon the monomer polymerization on the AgNPs/POM/rGO coated GCE, which indicated significant blocking effects caused by the formed MIP film. Upon the removal of the creatinine from MIP/AgNPs/POM/rGO coated GCE, R_{ct} was reduced to *ca.* 362Ω , together with the appearance of the recognition sites of creatinine molecules. On the other hand the R_{ct} was increased up to 463Ω after the creatinine was rebinded. These data indicate that the presence of creatinine molecules hinders the electrochemical reaction of $1.0 \text{ mM } [\text{Fe}(\text{CN})_6]^{3-/4-}$ on the electrode surface.

No DPV peak current was shown at MIP/AgNPs/POM/rGO coated GCE in PBS (0.1 M, pH 6.0), as displayed in Fig. 3C and Fig. 3D. The peak current reached *ca.* 1.25 V after 1.5 nM creatinine was rebinded. However, an insignificant peak current was observed at NIP/AgNPs/POM/rGO coated GCE, due to the non-specific interaction. DPV measurement was carried out using varying GCEs to study their current signals for comparison. Compared with the MIP coated GCE, MIP/rGO coated GCE, MIP/POM/rGO coated GCE, the MIP/AgNPs/POM/rGO coated

GCE exhibited more enhanced current signals, which resulted from its large surface area. It is worth mentioning that POMs, molecular components with high redox-activity, could be potentially used for sensor fabrication and electrochemical energy storage. In reduced forms, their electron and proton transfer and/or storage abilities allow them to act as efficient donors or acceptors of multiple electrons without structural change. Owing to their chemical versatility, POMs have been employed in catalysis, energy conversion and electronics [42, 43]. For the POMs, the reactivity and structure of could be significantly adjusted, since this kind of anionic metal oxides were based on high-valent transition metals.

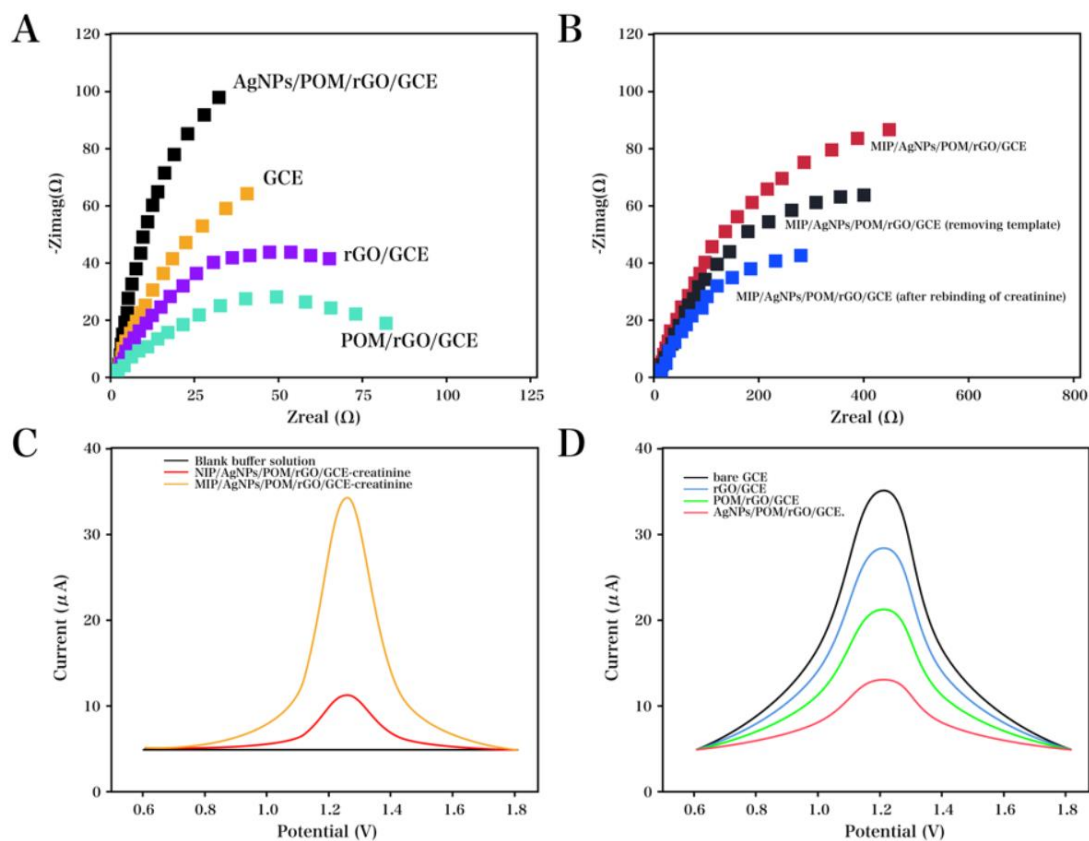


Figure 3. (A) EIS profile recorded for the bare GCE, rGO coated GCE, POM/rGO coated GCE and AgNPs/POM/rGO coated GCE coated GCE in 1.0 mM $[\text{Fe}(\text{CN})_6]^{3-/4-}$ solution in 0.1 M KCl, (B) EIS profile recorded for MIP/AgNPs/POM/rGO coated GCE, MIP/AgNPs/POM/rGO coated GCE (without template) and MIP/AgNPs/POM/rGO coated GCE (after rebinding of creatinine) in 1.0 mM $[\text{Fe}(\text{CN})_6]^{3-/4-}$ solution in 0.1 M KCl, (C) DPV curves recorded for varying electrodes in 0.1 M pH 6.0 PBS: MIP/AgNPs/POM/rGO coated GCE in blank buffer solution, NIP/AgNPs/POM/rGO coated GCE after rebinding of 1.5 nM creatinine, MIP/AgNPs/POM/rGO coated GCE after rebinding of 1.5 nM creatinine, (D) DPVs recorded for varying MIP electrodes in 0.1 M pH 6.0 PBS after rebinding of 1.5 nM creatinine: the bare GCE, rGO coated GCE, POM/rGO coated GCE and AgNPs/POM/rGO coated GCE.

A linear relationship was found between the increase in creatinine amount and the signal increase, as shown in the voltammograms in Fig. 4 obtained using increased concentrations of OCH. The calibration curve corresponded to the mean value of six experiments. The limit of detection (LOD)

was calculated as 0.0151 nM. To allow for comparison to previous reports, the characteristics of different electrochemical sensors for creatinine are summarized in Table 1.

Three independently prepared AgNPs/POM/rGO coated GCEs were used to measure their responses toward creatinine (1.0 nM) so as to study the interelectrode reproducibility. And the relative standard deviation (RSD) was obtained as 3.9%, which suggested that the reproducibility of the proposed electrode was desirable. After five measurements, the repeatability of our proposed bio sensor toward the adsorption of creatinine (1.0 nM) was determined so as to study the response, with an RSD of *ca.* 4.4%, which indicated that the proposed biosensor was highly repeatable.

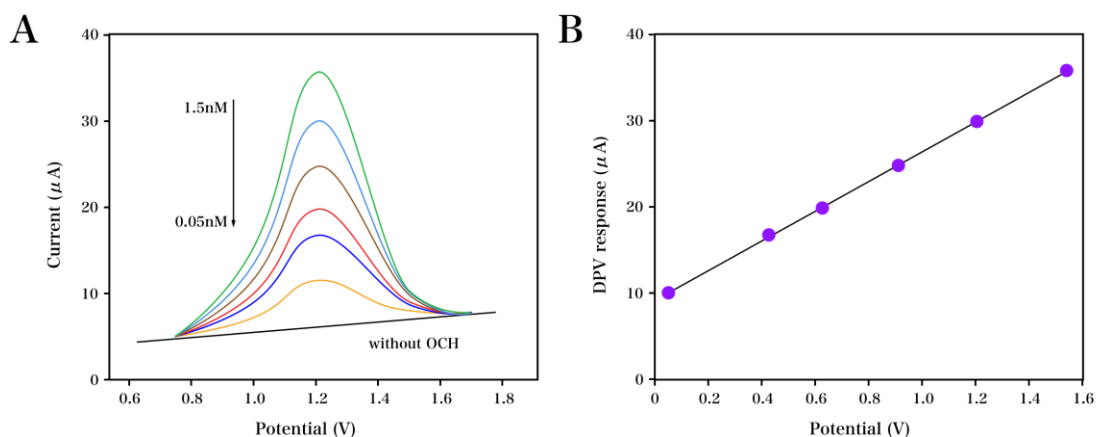


Figure 4. (A) DPV curves recorded for the developed voltammetric sensor with varying amount of creatinine in PBS (pH 6.0); (B) the calibration curve recorded for creatinine.

Table 1. Comparison of the major characteristics of electrochemical sensors used for the detection of creatinine.

Electrode	Linear detection range	Detection limit	Reference
Poly(ethyleneimine)/phosphotungstic acid multilayer modified electrode	0.125 to 62.5 µM	0.06 µM	[44]
Ni@PANI-modified GCE	40-800 nM	0.2 nM	[45]
Poly(methylvinyl ether)/maleic anhydride modified by esterification	-	-	[46]
MIP/AgNPs/POM/rGO coated GCE	0.05 – 1.5 nM	0.0151 nM	This work

Interfering substances including NaCl, insulin (Ins), urea, ferritin (fer), uric acid (UA), globulin (Glo), albumin (Alb), lysine (Lys), histidine (His), glutamic acid (GA), arginine (Arg), tyrosine (Tyr), citric acid (CA), and a mixture of these substances were used to study the selectivity of the AgNPs/POM/rGO coated GCE toward the detection of creatinine through DPV responses. At the AgNPs/POM/rGO coated GCE, a current response was observed for creatinine and the aforementioned substances. Moreover, the stability of the sensor was studied by detecting creatinine after the sensor was stored at 4 °C for 10 days without use. After the first two weeks, there was no obvious decrease in the initial response. After 10 days, approximately 90% of the initial current remained. On the other

hand, after water washing, the interfering agents showed almost no response, whereas response could still be observed at creatinine, which suggested that water washing could easily eliminate some non-specific binding of the analyte molecules. Furthermore, after the addition of interference substances into creatinine, a full current response was recorded for the target creatinine molecule at our proposed biosensor. For the bare electrode, the current height and peak potential recorded for tyrosine and citric acid were comparable with that for creatinine. The level analysis of creatinine in serum and saliva specimens were also carried out. The developed biosensor was highly accurate toward the determination of creatinine, as indicated in Table 1.

Table 2. Recoveries of the developed sensor toward the analysis of creatinine in saliva and serum.

Sample	Added (nM)	Found (nM)	Recovery (%)	RSD (%)
Saliva 1	0.50	0.45	89.4	2.86
Saliva 2	1.00	1.04	104.1	3.01
Serum 1	0.50	0.50	100.4	2.78
Serum 2	1.00	0.97	97.4	4.07

4. CONCLUSIONS

In the present study, a AgNPs/POM /rGO based creatinine imprinted voltammetric biosensor was proposed for the detection of OCH in wine and grape juice. Several different methods were used for the characterization of the nanomaterials. It can be seen that the proposed biosensor was highly sensitive for the detection of creatinine, and the LOD was calculated as 1.51×10^{-11} M. Furthermore, this MIP biosensor showed desirable stability and sensitivity. Therefore the proposed sensor could be potentially used for routine detection of creatinine in food specimens.

References

1. C. Magri, R. Xuereb and S. Fava, *Cardiology*, 129 (2014) 28.
2. P. Triska, P. Soares, E. Patin, V. Fernandes, V. Cerny and L. Pereira, *Genome Biology & Evolution*, 7 (2015) 3484.
3. S. Salvatore, M. Troxell, D. Hecox, K. Sperling and S. Seshan, *American Journal of Nephrology*, 41 (2015) 66.
4. O. Oruç Alper, O. Didem, O. Fatih, G. Murat and T. Kultigin, *Cardiorenal Medicine*, 6 (2016) 216.
5. H. Nobakht, T. Malakoutian, M. Radfar, E. Abdi, M. Kamgar, B. Broumand and I. Fazel, *Iranian Journal of Kidney Diseases*, 9 (2015) 273.
6. M. Ueda, K. Uchimura, Y. Narita, Y. Miyasato, T. Mizumoto, J. Morinaga, M. Hayata, Y. Kakizoe, M. Adachi and T. Miyoshi, *Nephron*, 129 (2015) 223.
7. J. Stephen, T. Anderson-Haag, S. Gustafson, J. Snyder, B. Kasiske and A. Israni, *American Journal of Nephrology*, 40 (2014) 546.
8. J. Rosman, A. Donker, S. Meijer, W. Sluiter, T. Piersbecht and d.H.G.K. Van, *Contributions to Nephrology*, 53 (2015) 109.
9. P. Björntorp, *Magnetic Resonance in Chemistry Mrc*, 13 (2015) 295.

10. S. Springer, J. Silverstein, K. Copeland, K. Moore, G. Prazar, T. Raymer, R. Shiffman, V. Thaker, M. Anderson and S. Spann, *Pediatrics*, 131 (2013) e648.
11. M. Cohen-Wolkowicz, D. Ouellet, P. Smith, L. James, A. Ross, J. Sullivan, M. Walsh, A. Zadell, N. Newman and N. White, *Antimicrobial Agents & Chemotherapy*, 56 (2012) 1828.
12. F. Rader, D. Wagoner, P. Ellinor, A. Gillinov, M.K. Chung, O. Costantini and E. Blackstone, *Circulation Arrhythmia & Electrophysiology*, 4 (2011) 644.
13. P. Jaganmohan, S. Rao and K. Rao, *World Journal of Medical Sciences*, 5 (2010) 45.
14. M. Miyake, A. Shibukawa and T. Nakagawa, *Journal of Separation Science*, 14 (2015) 181.
15. M. Kosikowski and Z. Suszyński, *Journal of Separation Science*, 35 (2012) 436.
16. A. Benkert, F.W. Scheller, W. Schoessler, B. Micheel and A. Warsinke, *Electroanalysis*, 12 (2015) 1318.
17. C. Chen and M. Lin, *Biosensors & bioelectronics*, 31 (2012) 90.
18. S. Wang, X. Li, J. Yang, X. Yang, F. Hou and Z. Chen, *Chroma*, 75 (2012) 1287.
19. K. Talalak, J. Noiphung, T. Songjaroen, O. Chailapakul and W. Laiwattanapaisal, *Talanta*, 144 (2015) 915.
20. M. Fernandezfernandez, P. Rodriguezgonzalez, M. Añónalvarez, F. Rodríguez, F. Menéndez and J. Alonso, *Anal. Chem.*, 87 (2015) 4053.
21. R. Matsui, T. Sakaki and T. Osakai, *Electroanalysis*, 24 (2012) 2325.
22. M. Alula and J. Yang, *Talanta*, 130 (2014) 55.
23. M. Suzuki, M. Furuhashi, S. Sesoko, K. Kosuge, T. Maeda, K. Todoroki, K. Inoue, J.Z. Min and T. Toyo'Oka, *Anal. Chim. Acta.*, 911 (2016) 92.
24. D. Liang, X. Fang, M. Li, K. Chingin and H. Li, *Analytical Letters*, 48 (2015) 2002.
25. P. Han, S. Xu, S. Feng, Y. Hao and J. Wang, *Talanta*, 151 (2016) 114.
26. J. Sitanurak, P. Inpota, T. Mantim, N. Ratanawimarnwong, P. Wilairat and D. Nacapricha, *The Analyst*, 140 (2015) 295.
27. A. Kozitsina, S. Dedeneva, Z. Shalygina, A. Okhokhonin, D. Chizhov, A. Matern and K. Brainina, *Journal of Analytical Chemistry*, 69 (2014) 758.
28. P. Shaw, *Analytical Letters*, 47 (2014) 689.
29. R. Šigutová, M. Hladík, F. Všianský, P. Kušnierová, K. Šafarčík and J. Tomandl, *Chemické Listy*, (2013) S444.
30. M. Yola, T. Eren and N. Atar, *Sensors and Actuators B: Chemical*, 210 (2015) 149.
31. V. Gupta, M. Yola, N. Özaltın, N. Atar, Z. Üstündağ and L. Uzun, *Electrochimica Acta*, 112 (2013) 37.
32. Y. Kim and S. Shanmugam, *ACS applied materials & interfaces*, 5 (2013) 12197.
33. T. Eren, N. Atar, M.L. Yola, H. Karimi-Maleh, A.T. Çolak and A. Olgun, *Ionics*, 21 (2015) 2193.
34. M. Yola, V. Gupta and N. Atar, *Materials Science & Engineering C*, 61 (2016) 368.
35. F. Lorestani, Z. Shahnava, P. Mn, Y. Alias and N. Manan, *Sensors & Actuators B Chemical*, 208 (2015) 389.
36. N. Atar, T. Eren, B. Demirdögen, M. Yola and M. Çağlayan, *Ionics*, 21 (2015) 2285.
37. P. Nia, F. Lorestani, W. Meng and Y. Alias, *Appl. Surf. Sci.*, 332 (2015) 648.
38. S. Gurunathan, J. Han, J. Park, E. Kim, Y. Choi, D. Kwon and J. Kim, *International Journal of Nanomedicine*, 10 (2015) 6257.
39. A.. Dwivedi, S. Dubey, M. Sillanpää, Y. Kwon, C. Lee and R. Varma, *Coordination Chemistry Reviews*, 287 (2015) 64.
40. H. Mehl, M. Oliveira and A. Zarbin, *Journal of Colloid and Interface Science*, 438 (2015) 29.
41. Q. Huang, J. Wang, W. Wei, Q. Yan, C. Wu and X. Zhu, *J. Hazard. Mater.*, 283 (2015) 123.
42. Y. Song and R. Tsunashima, *Chemical Society Reviews*, 41 (2012) 7384.
43. Y. Ji, T. Li and Y. Song, *Ind. Eng. Chem. Res.*, 53 (2014) 11566.
44. P. Han, S. Xu, S. Feng, Y. Hao and J. Wang, *Talanta*, 151 (2016) 114.
45. H. Rao, Z. Lu, H. Ge, X. Liu, B. Chen, P. Zou, X. Wang, H. He, X. Zeng and Y. Wang, *Microchim.*

Acta., 25 (2017) 145.

46. W. Ho, S. Krause, C. Mcneil, J. Pritchard, R. Armstrong, D. Athey and K. Rawson, *Anal. Chem.*, 71 (1999) 1940

© 2018 The Authors. Published by ESG (www.electrochemsci.org). This article is an open access article distributed under the terms and conditions of the Creative Commons Attribution license (<http://creativecommons.org/licenses/by/4.0/>).